



Exergy-Economic Optimization of Gasket-Plate Heat Exchangers

Sayed Ehsan Alavi, Meisam Moori Shirbani*, Mohammad Koochak Tondro

Faculty of Engineering, Shohadaye Hoveizeh Campus of Technology, Shahid Chamran University of Ahvaz, Dashte Azadegan, Iran.

Abstract

In this research, using Harris Hawks optimization method, the gasket- plate heat exchangers is studied with an exergy- economic approach. Six parameters of hot fluid inlet temperature, cold fluid inlet temperature, hot fluid mass flow rate, cold fluid mass flow rate, port diameter and the number of plates were selected as design variables. The ratio of hot fluid mass flow rate to cold fluid mass flow rate, λ , is introduced to the analysis of exergy loss. The results showed that using Harris Hawks optimization method, exergy loss and total cost can be reduced by 70% and 81%, respectively. The optimization results showed that minimizing the exergy loss, the efficiency of the gasket- plate heat exchanger increases by 30%. It is also found that for $\lambda > 1$, with the increase of cold fluid mass flow rate, the exergy loss number decreases and for $\lambda < 1$, with the increase of cold fluid mass flow rate, the exergy loss number increases.

Keywords: Gasket-plate heat exchanger, Exergy loss, Cost, Efficiency, Heat transfer.

1. Introduction

Considering the limitation of energy resources, the increase in demand for energy consumption and the presence of significant losses in thermal systems, it is necessary to provide a solution to reduce energy loss from these systems. There are two important irreversibility factors in heat exchangers; one is heat conduction due to limited temperature difference and the other is fluid friction. The number of entropic potential losses is caused by the irreversibility of the heat transfer process [1].

In their research, Yusuf A. Al-Turki et al. [2] studied plate heat exchangers with non-parallel plates. The results of this investigation showed that Nusselt number and thermal efficiency are higher in plate heat exchangers with non-parallel plates compared to heat exchangers with parallel plates. In this study, they also analyzed and compared the second law of thermodynamics for heat exchangers with parallel and non-parallel plates. Vikas Kumar et al. [3] investigated the effect of hybrid nanofluids $Al_2O_3 + MWCNT/water$, $TiO_2 + MWCNT/water$, $ZnO + MWCNT/water$, $CeO_2 + MWCNT/water$ on exergetic efficiency in plate heat exchangers. In their research, they found that using hybrid nanofluid $CeO_2 + MWCNT/water$, the greatest reduction in exergy loss is achieved. Bejan [4, 5] defined and minimized the total rate of entropy generation as the sum of the entropy produced due to the limited temperature difference and frictional pressure drop of the fluid. Minimizing the produced entropy is used in many thermodynamic analyzes and heat exchangers optimization. Since in the analysis of heat exchangers, efficiency is a more important parameter than heat transfer, in some cases contradictions are observed. The results of this research showed that the principle of minimizing entropy generation is more useful in optimizing heat exchangers whose purpose is to convert heat into work [6]. Chen et al. [7] minimized entropy generation and entransy dissipations separately minimized the generation entropy and entropy losses separately for a four square cavity. They found that minimizing the entropy generation causes the maximum amount of heat to be converted into work in the heat exchangers, while minimizing the entransy dissipations maximizes the efficiency. Ghodoossi et al. [8] using the method of minimizing entropy generation analyzed the effect of the complex levels of tree networks on the heat conduction paths and came to the conclusion that if the complex levels of heat generation increase, basically the performance of the heat flow does not improve. Escher et al. [9] showed in their research that the performance

* Corresponding author. Tel.: 989166054534; E-mail address: m.mooryshirbani@scu.ac.ir

coefficient of parallel channels network is more than 5 times that of tree networks with constant mass flow rate. This is while almost 4 times more heat is taken from tree networks in the constant pressure gradient. Therefore, the efficiency of the heat exchanger does not always increase by reducing the entropy generation. In their research, Liu et al. [10] minimized entropy generation and entransy dissipations. From the comparison of the results, they found that the optimization of heat exchangers in heat transfer processes such as the Brayton cycle, whose main goal is to convert heat into work, by minimizing the entropy generation, has better results. Shah and Skiepko [11] studied the relationship between entropy generation and efficiency for 18 types of heat exchangers. The results showed that in some cases minimizing the entropy generation, not only the efficiency of the heat exchanger did not increase but also decreased. Therefore, they found that minimizing the entropy generation does not necessarily optimize the heat exchanger. Cao et al. [12] numerically simulated the effect of the spiral baffle angle of heat exchangers on the resistance to fluid flow and heat transfer. The experimental results showed that the performance of the heat exchanger increases with the increase of the spiral angle of the baffle. Jamil et al. [13] presented a numerical model. In their research and analyzed gasket-plate heat exchangers with a thermal-hydraulic view. They showed that the flow rate and Chevron angle are very influential on the pressure drop and heat transfer. Also, they found that they make the fouling resistance very accurate in the design of the heat exchanger. Jutapatet et al. [14] investigated the effect of surface roughness on the condensation of R-134A in gasket-plate heat exchangers. The results showed that the heat transfer coefficient of the rough surface is 31 to 41% higher than that of the smooth surface. While the frictional pressure gradient of the rough surface is about 14 to 29% higher than that of the smooth surface. Finally, they introduced the rough surface as a suitable alternative to smooth surfaces. Nahes et al. [15] presented an optimal design method for gasket-plate heat exchangers called Set Trimming for the first time. The innovation of the method introduced in this research was the reduction of the search space, which guaranteed convergence and did not depend on good initial guesses. In their research, they showed that the Set Trimming method is faster than other methods in designing a plate heat exchanger. Soman et al. [16] using Solidworks software studied the effect of hot and cold fluid flow on heat transfer parameters. In this research, water was chosen as the working fluid, and firstly, the effect of hot fluid flow rate on Nusselt number was studied. Next, the effect of Reynolds number of hot fluid on Nusselt number of cold fluid was investigated. The results showed that increasing the speed of the hot fluid flow increases the Nusselt number. It was also observed that increasing the Reynolds number of hot fluid increases the Nusselt number of cold fluid. Kumar et al. [17] studied the effect of geometrical parameters on the performance of Chevron plate heat exchangers. In this research, the effect of the Chevron angle on the friction factor, pressure drop and efficiency of the heat exchanger was investigated experimentally. The results showed that a higher Chevron angle leads to a uniform distribution of the fluid flow in the channel and an increase in the efficiency of the heat exchanger. Zhong et al. [18] experimentally and numerically investigated the hydraulic performance of plate heat exchangers at low Reynolds numbers. The results showed that the pressure drop of the studied plate heat exchanger increases with the increase of Reynolds number and temperature, while the friction factor of the plate heat exchanger decreases with the increase of Reynolds number, but is not affected by temperature. Guo et al. [19] modeled the plate heat exchanger based on sensitivity analysis. Compared to other models, the model presented in this research is modeled in less time and also has the ability to track the temperature of the outlet cooling water with high accuracy in different operating conditions of the heat exchanger. The presented model can be used to save and optimize the energy of the circulating cooling water systems. Other similar researches in the field of nano, vibrations and buckling can be accessed in the references.

A review of previous works shows that the relationship between exergetic efficiency and thermal efficiency in heat exchangers has been studied in most researches. Optimization of gasket-plate heat exchangers with an exergy-economic point of view is the aim of this study. The ratio of hot fluid mass flow rate to the cold fluid mass flow rate is very important in exergy and thermodynamic analysis of gasket-plate heat exchangers, which is comprehensively investigated in this research. Also, the effect of the inlet and outlet temperatures of hot and cold fluids on the exergy loss number is studied.

2. Exergy-Economic modelling

In this research, a gasket-plate heat exchanger with opposite flow direction and Chevron plates is investigated; a schematic of its plates is shown in Figure 1.

The research assumptions are:

- The condition is steady state.
- The overall heat transfer coefficient is constant throughout the length of the heat exchanger.
- The flow of hot and cold fluids is uniform in all directions.
- Heat loss is negligible.

- The temperature of hot and cold fluids is uniform.
- The velocity in the cross section of the inlet and outlet flow is uniform.
- The fouling resistance is assumed to be constant.

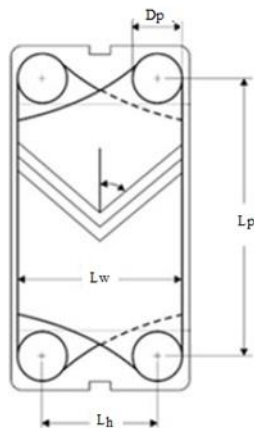


Figure1: Schematic of gasket- plate heat exchanger.

The efficiency of a counter flow heat exchanger is expressed as follows [20]:

$$\varepsilon = \frac{1 - e^{-NTU(1-C^*)}}{1 - C^*e^{-NTU(1-C^*)}} \quad (1)$$

In equation (1), the number of transfer units and the heat capacity ratio are defined as follows [20]:

$$NTU_{max} = \frac{UA_{tot}}{C_{min}} \quad (2)$$

$$C^* = \frac{C_{min}}{C_{max}} \quad (3)$$

The overall heat transfer coefficient in the heat exchanger is [20]:

$$U = R_{f,h} + R_{f,c} + \left[\frac{1}{h_h} + \frac{1}{h_c} \right] + \left(\frac{t}{k} \right)_w \quad (4)$$

Where w, t and k refer to wall thickness and wall conductivity coefficient, respectively. The Nusselt number for both hot and cold fluids is obtained from the following equation [21]:

$$Nu = (Re)^{0.663} Pr^{1/3} \quad (5)$$

The heat transfer coefficient for both sides is obtained using the definition of Nusselt number as follows [21]:

$$h = \frac{Nu \times k}{de} \quad (6)$$

In the above equation, k is the heat transfer coefficient of the fluid conduction and de is the diameter of the Chevron plate, which obtained from the following relation [22]:

$$d_e = 2 \times b \quad (7)$$

$$b = p - t \quad (8)$$

Where p and b are the pitch plate and average distance, respectively. The Reynolds number of the cold and hot sides is obtained from the following equation [22]:

$$Re = \frac{G_{ch} \times d_e}{\mu} \tag{9}$$

G_{ch} is the mass flux that passes through each channel and is defined by the following equation [22]:

$$G_{ch} = \frac{\dot{m}_{ch}}{A_{ch}} \tag{10}$$

$$A_{ch} = b \times L_w \tag{11}$$

$$L_w = L_h + d_p \tag{12}$$

L_h and d_p are the horizontal distance taken from the center of the port and port diameter respectively. \dot{m}_{ch} is the mass flow rate that passes through each channel and is calculated from the following equation [20]:

$$\dot{m}_{ch} = \frac{\dot{m}}{n_{cp}} \tag{13}$$

$$n_{cp} = \frac{n_t - 1}{2 \times n_p} \tag{14}$$

n_{cp} is the number of channels in each pass. n_p and n_t are passes number and plates number, respectively. Length intensive plate is obtained from the following equation [20]:

$$L_c = n_t \times p \tag{15}$$

The total pressure drop in hot and cold fluids is obtained from the sum of the frictional pressure drop in the channel and the pressure drop in the port [20]:

$$\Delta p_{tot} = \Delta p_c + \Delta p_p \tag{16}$$

The frictional pressure drop in the channel is calculated from the following equation [20]:

$$\Delta p_c = \frac{4fL_v n_p G_{ch}^2}{2\rho d_e} \tag{17}$$

The friction factor for both hot and cold fluids is [20]:

$$f = \frac{1.441}{Re^{0.206}} \tag{18}$$

The pressure drop in the port expressed as [20]:

$$\Delta p_p = \frac{1.4n_p G_p^2}{2\rho} \tag{19}$$

$$L_v = L_p + d_p \tag{20}$$

$$L_p = \frac{A_{1p}}{L_w} \tag{21}$$

$$A_{1p} = \frac{A_1}{\emptyset} \tag{22}$$

$$G_p = \frac{4\dot{m}}{\pi d_p^2} \quad (23)$$

d_p is port diameter and A_1 , ϕ , G_p and L_v plate heat transfer surface area, enlargement coefficient, port mass flux and chevron plate height, respectively.

Exergy loss in the gasket-plate heat exchanger is expressed as the following equation [21]:

$$E = T_{sur} \left\{ \dot{m} C_p \ln \frac{T_{out}}{T_{in}} \right\} \quad (24)$$

The exergy loss number is defined as equation (25)[21]:

$$N_{EPL} = \frac{E}{T_{sur} C_{min}} \quad (25)$$

The total cost of gasket-plate heat exchanger includes initial capital cost and the operating cost includes the pumping cost can be given in following equations [22]:

$$C_{total} = C_{in} + C_{op} \quad (26)$$

The operating cost C_{op} and the initial investment C_{in} for the plates with stainless steel (SS 304) can be obtained as follows [22]:

$$p = \left(\frac{\dot{m}_t \Delta p_t}{\rho_t} + \frac{\dot{m}_s \Delta p_s}{\rho_s} \right) \frac{1}{\eta} \quad (27)$$

$$C_o = p * Kel * H \quad (28)$$

$$C_{op} = \sum_{k=1}^{ny} \frac{C_o}{(1+i)^k} \quad (29)$$

$$C_{in} = 635.14 \times A_{tot}^{0.778} \quad (30)$$

where C_o is the annual current cost, ny lifetime, i is the annual inflation rate, kel is the unit price of electrical energy, P is pumping power, H is the hours of operation per year and η is the pumping efficiency.

Now C_{total} is considered as the objective function for optimal design. In this investigation, the equipment life is taken to be $ny = 10$ years; the inflation rate is $i = 10\%$; the price of electricity is $kel = 0.15$ \$/kWh and the working hours and pumping efficiency are $H = 7500$ h/year, $\eta = 0.6$, respectively.

3. Harris Hawks optimization method[23]

The Harris Hawks optimization method is a population-based optimization method and consists of three steps. The first step is called exploration. Candidate solutions in this method are Harris Hawks. The best candidate solution in each step is considered as the near-optimal answer. Harris Hawks randomly settle in some places to search for the target. In the Harris Hawks optimization method, prey is identified based on two techniques. A: hawks are sitting and waiting according to the position of other hawks and rabbits. B: hawks are randomly sitting on tall trees and waiting. The second step is the transition from exploration to exploitation. A prey's energy is significantly reduced during escape. To model this fact, the energy of a prey is modeled as follows:

$$E = 2E_0 \left(1 - \frac{t}{T} \right) \quad (31)$$

In the above equation, E , T and E_0 represent the escape energy of the prey, the maximum number of repetitions and the initial energy of the prey, respectively. In Harris Hawks optimization algorithm, in any iteration, E_0 changes

randomly in the interval (-1, 1).As the value of E_0 is less than zero, the physical concept is that the rabbit is physically more tired, and as its value is greater than zero, it means that the physical strength of the rabbit has increased. The amount of dynamic escape energy decreases during iterations. In this algorithm, if the escape energy is less than one, during the exploitation steps, the hawks use the neighborhood of the solutions to find the location of the rabbit. If the escape energy is not less than one, the exploration step is repeated.

The third step in Harris Hawks optimization method is exploitation. At this step, Harris Hawks make a surprise attack on the intended prey that was discovered in the previous step. Since the prey tries to escape from dangerous situations, hawks use different techniques for chasing. According to the behavior of the prey in pursuit and its skill in escaping, the attack finally ends by catching the prey that is surprised in a very short time.

Since the optimization method of Harris Hawks is a new and capable algorithm in optimization and compared to many older methods, it achieves the optimal value with higher accuracy in fewer iterations, so in this research this method has been used to optimize the objective function.

In this study, the total cost and exergy loss of gasket-plate heat exchanger are considered as two objective functions. The characteristics of hot and cold fluids and the range of design variables are shown in tables (1) and (2), respectively.

Table 1: Characteristics of hot and cold fluids.

Process information	Hot fluid (water)	cold fluid (water)
fluid density(kg/m ³)	985	995
specific heat (j/kg.K)	4183	4178
fluid viscosity(pa.s)	0.000509	0.000776
fluid thermal conductivity(W/m.K)	0.645	0.617
Prandtl number	3.31	5.19
Fouling Factor(m ² . W/K)	0.00005	0

Table 2: Range of optimization variables.

variable	Lower limit	Upper limit
n_t	100	300
d_p (mm)	0.1	0.4
\dot{m}_c (kg/s)	80	130
\dot{m}_h (kg/s)	100	150
$T_{c,i}$ (K)	285	295
$T_{h,i}$ (K)	330	345

4. Results

In table (3) in order to validate and confirm the simulated code for the gasket-plate heat exchanger, the obtained thermal and hydraulic parameters have been compared with the results in reference (52). As can be seen, the results of present research have good agreement with the mentioned reference.

Table 3: Comparison of the results of present research with the results of other reference.

Parameter	present study	Ref [24]
Re_h	13373	13366
Re_c	8886	8881.6

Nu_h	243.2641	243.4
Nu_c	215.5268	215.46
$U(W/m^2K)$	6528.7	6636

In Fig.2, the results of Harris Hawks multi-objective optimization method are shown on the pareto front. As can be seen, different points on the curve can be suggested to achieve the research goals. The results of three points A, B and C are shown in Table 4 as points with priority selection. Point A introduces the optimal state in which the exergy loss is the lowest possible, but the total cost of the heat exchanger is the highest at this point. Point B introduces the optimal state in which the total cost of the heat exchanger is the lowest possible, but the exergy loss at this point is the highest. Point C shows the optimal state where it can be said that both study goals have been achieved. At this point, both the exergy loss and the total cost of the heat exchanger have been significantly reduced. The authors suggest point C as the optimal point.

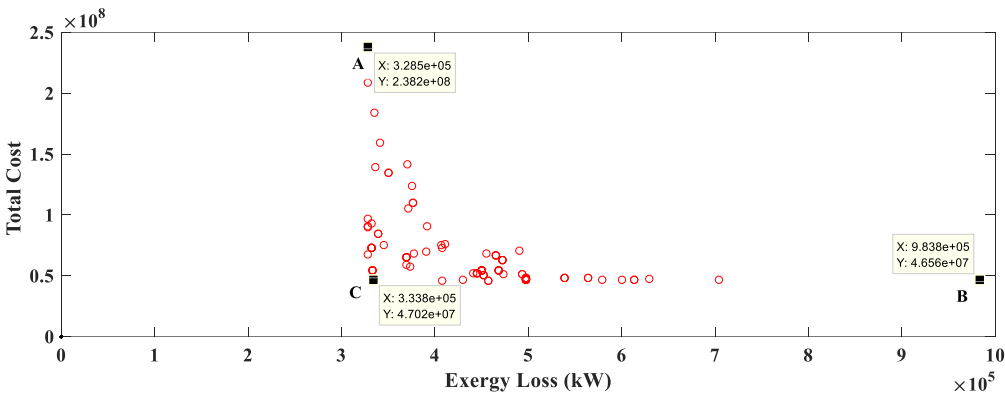


Figure 2:Optimized point's distribution in Pareto curve.

Table 4: Choosing optimized points on the Pareto front.

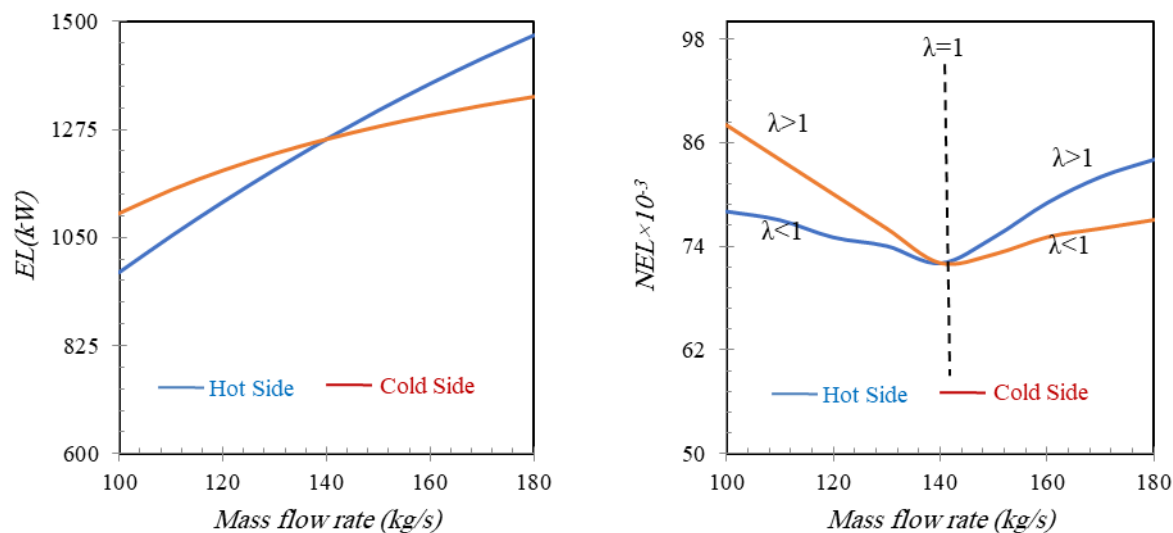
Choice	Exergy Loss (kW)	Total Cost(M\$)
A	328.5	238.2
B	983.8	46.56
C	333.8	47.02

Table 5 shows the design variables at point C and the optimization results in these conditions. It can be observed that the exergy loss and the exergy loss number have been reduced by 70% and 53%, respectively. Also, the optimization results showed that the efficiency of the heat exchanger has been increased by 30% and the total cost of the heat exchanger has been reduced by 81%.

Table 5: Comparison between optimum and initial values of design parameters.

variable	Initial values	Optimized values
n_t	105	300
d_p (mm)	0.2	0.3105
\dot{m}_c (kg/s)	140	80.5247
\dot{m}_h (kg/s)	140	100.6497
$T_{c,i}$ (K)	285	294.9581
$T_{h,i}$ (K)	338	330.088
Exergy Loss (kW)	1111.9	333.8
Total Cost (M\$)	245	47.02
Exergy Loss Number	0.007	0.0033
Efficiency (%)	55	85

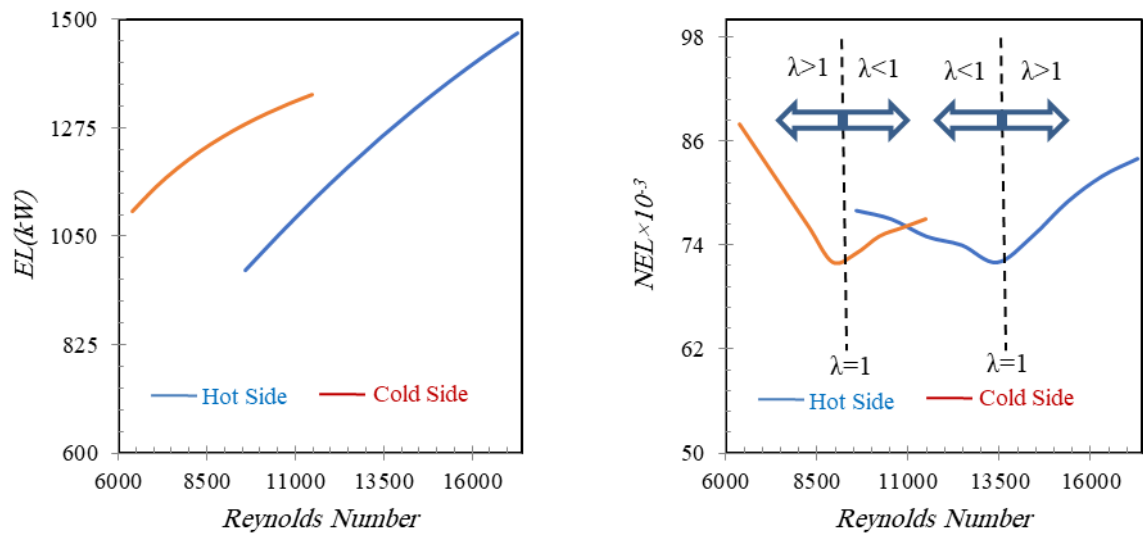
In this study, the effect of different parameters on the exergy loss is investigated in 3 cases: $\lambda=1$, $\lambda<1$ and $\lambda>1$. Fig.3(a) shows the effect of increasing the hot and cold fluids mass flow rate on exergy loss. It can be seen that the exergy loss increases with increasing the mass flow rate. It can also be found from the equation (24), the exergy loss has a direct relationship with the mass flow rate. Fig.3b shows the effect of increasing the hot and cold fluids mass flow rate on the exergy loss number. It can be observed that for $\lambda<1$, with the increase of hot fluid mass flow rate, the exergy loss number decreases and for $\lambda>1$, with the increase of hot fluid mass flow rate, the exergy loss number also increases. It is also seen that for $\lambda>1$, with the increase of cold fluid mass flow rate, the exergy loss number decreases and for $\lambda<1$, with the increase of cold fluid mass flow rate, the exergy loss number increases. The exergy loss number also depends on the minimum mass flow rate of hot and cold fluids. So, the results of Fig.3(a) will be different from Fig.3b. In the case of $\lambda<1$, the hot fluid mass flow rate will be the minimum mass flow rate. Therefore, in this case, the exergy loss number will have an inverse relationship with the hot fluid mass flow rate and a direct relationship with the cold fluid mass flow rate. In the case of $\lambda>1$, the other result of Fig.3(b) can be analyzed with a similar argument.



(a) (b)
Figure3: The effects of mass flow rate on a) exergy loss b) exergy loss number.

Fig.4 (a) shows the effect of increasing Reynolds number on exergy loss. It can be seen that increasing the Reynolds number, the exergy loss increases. The mass flow rate is directly related to the Reynolds number. On the other hand, the mass flow has a direct relationship with the exergy loss. Therefore, it can be concluded that the Reynolds number has a direct relationship with the exergy loss. Fig.4 (b) shows the effect of increasing the Reynolds number on the exergy loss number. It can be observed that different results have been obtained for different values of λ . It is found from the diagram that for hot fluid values of $\lambda<1$ and cold fluid values of $\lambda>1$, with

increasing the Reynolds number, the exergy loss number decreases. Also, the results show that for hot fluid values of $\lambda > 1$ and cold fluid values of $\lambda < 1$ with increasing the Reynolds number, the exergy loss number increases.



(a) (b)
Figure4: The effects of Reynolds number on a) exergyloss b) exergyloss number.

Fig.5 (a) shows the effect of increasing the fluid friction factor on the exergy loss. It can be observed that increasing the friction factor, the exergy loss decreases. The result can be justified in this way that, on the one hand, the Reynolds number has a direct relationship with the exergy loss, and on the other hand, according to the equation (18) between the Reynolds number and the fluid friction factor, it has an inverse relationship. Therefore, it can be concluded that the exergy loss has an inverse relationship with the fluid friction factor. Fig.5(b) shows the effect of increasing the friction factor on the exergy loss number. It can be found that, the hot fluid friction factor has an inverse relationship with the exergy loss number for $\lambda < 1$ and a direct relationship for $\lambda > 1$. Also, the results show that the cold fluid friction factor has a direct relationship with the exergy loss number for $\lambda < 1$ and an inverse relationship for $\lambda > 1$.

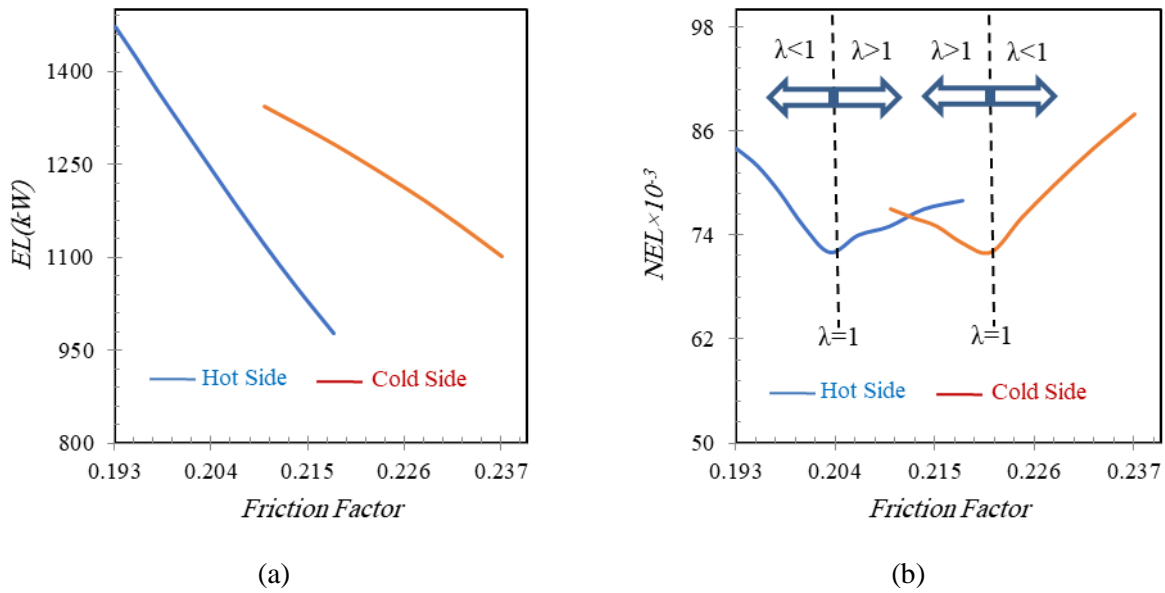


Figure5: The effects of friction factor on a) exergyloss b) exergyloss number.

The effect of increasing the hot fluid outlet temperature on the exergy loss for various values of λ is shown in Fig.6. It can be seen that increasing the hot fluid outlet temperature, the exergy loss has increased in some temperatures and decreased in some other temperatures, which is related to the comparison of the hot and cold fluid outlet temperatures. If the cold fluid outlet temperature is higher than the hot fluid outlet temperature, increasing the hot fluid outlet temperature, the exergy loss will increase. In other words, if the hot fluid outlet temperature is higher than the cold fluid outlet temperature, the exergy loss has an inverse relationship with the hot fluid outlet temperature. In both Figs. 6(a) and 6(b), it can be found that for $\lambda < 1$, the exergy loss and the exergy loss number decrease with the increase of hot fluid outlet temperature. Because for these values of λ , the cold fluid outlet temperature is always lower than the hot fluid outlet temperature. Also, from Fig. 6(a) it is observed that for $\lambda > 1$ with the increase of hot fluid outlet temperature, the exergy loss increases and then decreases. Because when the hot fluid outlet temperature is less than 315 K, the cold fluid outlet temperature is higher than the hot fluid outlet temperature.

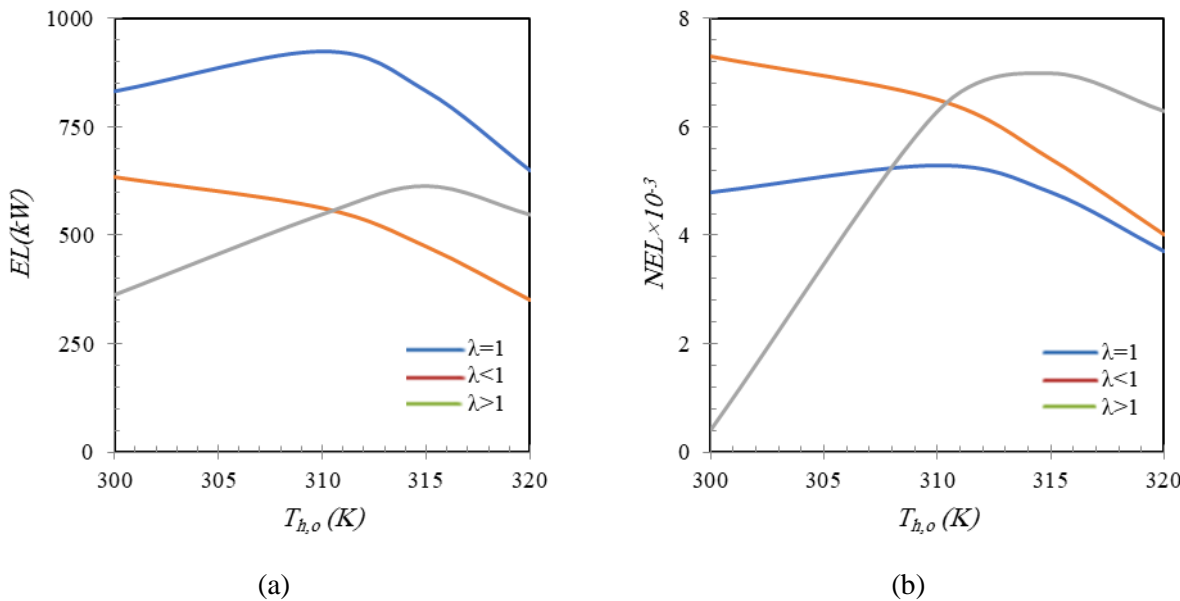


Figure 6: The effects of hot fluid outlet temperature on a) exergy loss b) exergy loss number.

The effect of increasing the hot fluid inlet temperature on the exergy loss for various values of λ is shown in Fig.7. It can be seen that for different values of λ , increasing the hot fluid inlet temperature causes an increase in the exergy loss and the exergy loss number. Also, the results of Fig.7 (a) show that at a given hot fluid inlet temperature, the highest value of exergy loss will occur for values of $\lambda=1$ and the lowest value of exergy loss will occur for values of $\lambda<1$. From the results of Fig.7(b), it can be found that at a given hot fluid inlet temperature, the lowest value of exergy loss number will occur for values of $\lambda=1$ and the highest value of exergy loss number will occur for values of $\lambda>1$.

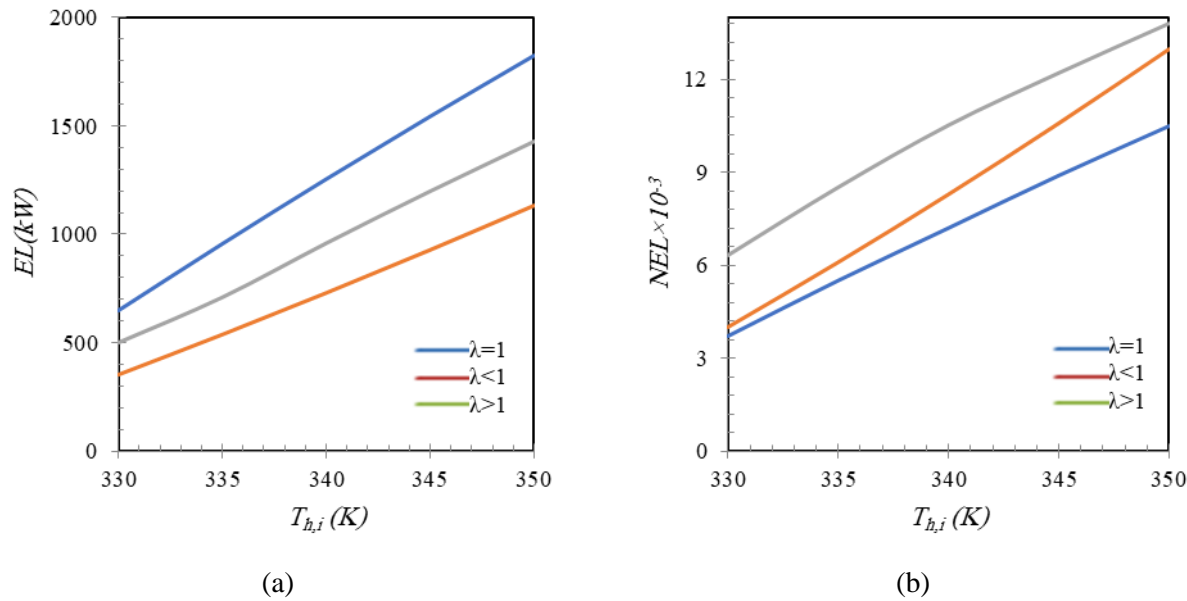
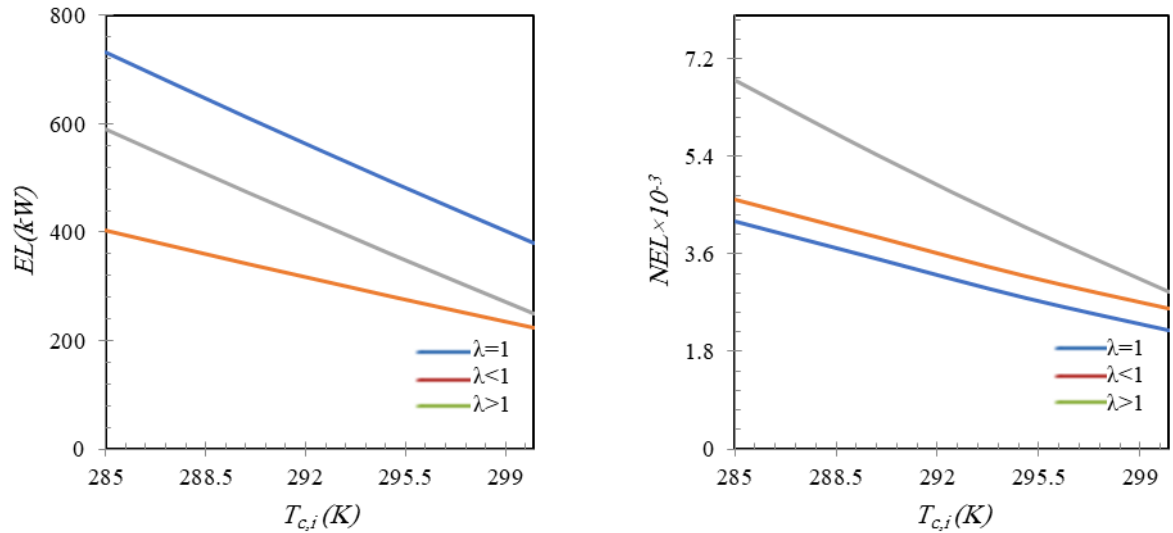


Figure 7: The effects of hot fluid inlet temperature on a) exergy loss b) exergy loss number.

The effect of increasing the cold fluid inlet temperature on the exergy loss for various values of λ is shown in Fig.8. It can be seen that for different values of λ , increasing the cold fluid inlet temperature causes a decrease in exergy loss and the exergy loss number. Also, it is obtained from Fig.8(a), at a given cold fluid inlet temperature, the highest value of exergy loss will occur for values of $\lambda=1$ and the lowest value of exergy loss will occur for values of $\lambda<1$. It can be found from the Fig. 8(b) at a given cold fluid inlet temperature, the lowest value of exergy loss number will occur for values of $\lambda=1$ and the highest value of exergy loss number will occur for values of $\lambda>1$.



(a) (b)
Figure 8: The effects of cold fluid inlet temperature on a) exergy loss b) exergy loss number.

5. Conclusion

In this research, minimizing exergy loss and total cost, a gasket-plate heat exchanger was optimized. Six parameters of hot fluid inlet temperature, cold fluid inlet temperature, hot fluid mass flow rate, cold fluid mass flow rate, port diameter and number of plates were selected as design variables. HarrisHawks optimization algorithm was used to optimize the heat exchanger. The results of exergy loss analysis were extracted for various values of the ratio of the hot fluid mass flow rate to the cold fluid mass flow rate. The important results of the study can be stated as follows:

- The optimization results showed that exergy loss and total cost can be reduced by 70% and 81%, respectively.
- Optimizing the gasket-plate heat exchanger, its efficiency increased by 30%.
- For hot fluid values of $\lambda > 1$ and cold fluid values of $\lambda < 1$ with increasing the Reynolds number, the exergy loss number increases.
- The hot fluid friction factor has an inverse relationship with the exergy loss number for $\lambda < 1$ and a direct relationship for $\lambda > 1$.
- At a given hot fluid inlet temperature, the lowest value of exergy loss number will occur for values of $\lambda = 1$ and the highest value of exergy loss number will occur for values of $\lambda > 1$.
- At a given cold fluid inlet temperature, the highest value of exergy loss will occur for values of $\lambda = 1$ and the lowest value of exergy loss will occur for values of $\lambda < 1$.

Nomenclature			
A	Overall heat transfer area	N	Nusselt number (-)
		u	
(m^2)		P	Plates pitch (m)
		Pr	Prandtl number (-)
A_{ch}	Channel flow area (m^2)	q	Heat transfer rate (w)
A_1	Heat transfer area of a plate (m^2)	R	Reynolds number(-)
		e	
b	Average distance (m)	R_f	Fouling resistance(m^2kw-1)
C_p	Specific heat capacity (J/kg.K)	T	Temperature (K)
C^*	Heat capacity ratio(-)	t	Plate thickness (m)
d_e	Equivalent diameter (m)	U	Overall heat transfer coefficient ($W/m^2.K$)
d_p	Port diameter (m)	Greek abbreviation	
f	friction coefficient(-)	ΔP	Pressure drop (kPa)
G_{ch}	Mass flux in each channel ($kg/m^2.s$)	μ	Viscosity (Pa.s)
G_p	Mass flux in the ports ($kg/m^2.s$)	ρ	Density (kg/m^3)
h	Convection heat transfer coefficient ($W/m^2.K$)	ε	Effectiveness(-)
K	Conductive heat transfer coefficient (W/m.K)	ϕ	Enlargement coefficient (-)
L_v	Chevron plate height (m)	β	Chevron angle of plates(degree)

L_h	Horizontal distance in openings (m)		<i>Subscripts</i>
L_p	Heat exchanger plate height (m)	h	Hot
L_w	Plate width (m)	c	Cold
L_c	Length intensive of plates (m)	c	Channel
		h	
\dot{m}	Mass flow rate (kg/s)	i	input
\dot{m}_{ch}	Mass flow rate in each channel (kg/s)	o	output

6. References

[1] M. Chahartaghi, S. E. Alavi, A. J. J. o. C. A. M. Sarreshtehdari, Investigation of energy consumption reduction in multistage compression process and its solutions, Vol. 50, No. 2, pp. 219-227, 2019.

[2] Y. A. Al-Turki, H. Moria, A. Shawabkeh, S. Pourhedayat, M. Hashemian, H. S. J. C. E. Dizaji, P.-P. Intensification, Thermal, frictional and exergetic analysis of non-parallel configurations for plate heat exchangers, Vol. 161, pp. 108319, 2021.

[3] V. Kumar, A. K. Tiwari, S. K. J. M. R. E. Ghosh, Exergy analysis of hybrid nanofluids with optimum concentration in a plate heat exchanger, Vol. 5, No. 6, pp. 065022, 2018.

[4] A. Bejan, 2013, *Entropy generation minimization: the method of thermodynamic optimization of finite-size systems and finite-time processes*, CRC press,

[5] A. Bejan, J. Kestin, Entropy generation through heat and fluid flow, 1983.

[6] J. Hesselgreaves, Rationalisation of second law analysis of heat exchangers, *International Journal of Heat and Mass Transfer*, Vol. 43, No. 22, pp. 4189-4204, 2000.

[7] Q. Chen, M. Wang, N. Pan, Z.-Y. J. E. Guo, Optimization principles for convective heat transfer, Vol. 34, No. 9, pp. 1199-1206, 2009.

[8] L. J. E. c. Ghodoossi, management, Entropy generation rate in uniform heat generating area cooled by conducting paths: criterion for rating the performance of constructal designs, Vol. 45, No. 18-19, pp. 2951-2969, 2004.

[9] W. Escher, B. Michel, D. J. I. J. o. H. Poulikakos, M. Transfer, Efficiency of optimized bifurcating tree-like and parallel microchannel networks in the cooling of electronics, Vol. 52, No. 5-6, pp. 1421-1430, 2009.

[10] X. Liu, J. Meng, Z. Guo, Entropy generation extremum and entransy dissipation extremum for heat exchanger optimization, *Chinese Science Bulletin*, Vol. 54, No. 6, pp. 943-947, 2009.

[11] R. K. Shah, T. J. J. H. T. Skiepko, Entropy generation extrema and their relationship with heat exchanger effectiveness—Number of transfer unit behavior for complex flow arrangements, Vol. 126, No. 6, pp. 994-1002, 2004.

[12] B. Gao, Q. Bi, Z. Nie, J. J. E. t. Wu, f. Science, Experimental study of effects of baffle helix angle on shell-side performance of shell-and-tube heat exchangers with discontinuous helical baffles, Vol. 68, pp. 48-57, 2015.

[13] M. A. Jamil, Z. U. Din, T. S. Goraya, H. Yaqoob, S. M. J. E. C. Zubair, Management, Thermal-hydraulic characteristics of gasketed plate heat exchangers as a preheater for thermal desalination systems, Vol. 205, pp. 112425, 2020.

[14] J. Soontarapiromsook, O. Mahian, A. S. Dalkilic, S. J. E. T. Wongwises, F. Science, Effect of surface roughness on the condensation of R-134a in vertical chevron gasketed plate heat exchangers, Vol. 91, pp. 54-63, 2018.

[15] A. L. Nahes, N. R. Martins, M. J. Bagajewicz, A. L. J. I. Costa, E. C. Research, Computational study of the use of set trimming for the globally optimal design of gasketed-plate heat exchangers, Vol. 60, No. 4, pp. 1746-1755, 2021.

[16] D. P. SOMAN, V. DT, T. J. I. J. o. C. RADHAKRISHNAN, C. Engineering, Computational Fluid Dynamics Modelling and Analysis of Heat Transfer in Multichannel Dimple Plate Heat Exchanger, 2021.

[17] B. Kumar, A. Soni, S. J. E. T. Singh, F. Science, Effect of geometrical parameters on the performance of chevron type plate heat exchanger, Vol. 91, pp. 126-133, 2018.

- [18] Y. Zhong, K. Deng, S. Zhao, J. Hu, Y. Zhong, Q. Li, Z. Wu, Z. Lu, Q. J. P. Wen, Experimental and numerical study on hydraulic performance of chevron brazed plate heat exchanger at low Reynolds number, Vol. 8, No. 9, pp. 1076, 2020.
- [19] Y. Guo, F. Wang, M. Jia, S. J. C. E. R. Zhang, Design, Modeling of plate heat exchanger based on sensitivity analysis and model updating, Vol. 138, pp. 418-432, 2018.
- [20] H. Hajabdollahi, M. Naderi, S. J. A. T. E. Adimi, A comparative study on the shell and tube and gasket-plate heat exchangers: The economic viewpoint, Vol. 92, pp. 271-282, 2016.
- [21] H. S. Dizaji, S. Jafarmadar, M. J. E. Hashemian, The effect of flow, thermodynamic and geometrical characteristics on exergy loss in shell and coiled tube heat exchangers, Vol. 91, pp. 678-684, 2015.
- [22] M. Mehregan, S. E. J. E. E. Alavi, Systems, Thermal and economic optimization of an intercooler of three-stage compressor, Vol. 9, No. 3, pp. 261-278, 2021.
- [23] A. A. Heidari, S. Mirjalili, H. Faris, I. Aljarah, M. Mafarja, H. J. F. g. c. s. Chen, Harris hawks optimization: Algorithm and applications, Vol. 97, pp. 849-872, 2019.
- [24] S. Kakac, H. Liu, A. Pramuanjaroenkij, 2012, *Heat exchangers: selection, rating, and thermal design*, CRC press,